Materials Letters 68 (2012) 450–452

Contents lists available at SciVerse ScienceDirect

Materials Letters

journal homepage: www.elsevier.com/locate/matlet

Improved corrosion resistance of stainless steel 316L by Ti ion implantation

Kai Feng [a], Xun Cai [a,*], Zhuguo Li [a,*], Paul K. Chu [b]

[a] Shanghai Key laboratory of Materials Laser Processing and Modification, School of Materials Science and Engineering, Shanghai Jiao Tong University, Shanghai, China
[b] Department of Physics and Materials Science, City University of Hong Kong, Tat Chee Avenue, Kowloon, Hong Kong, China

ARTICLE INFO

Article history:
Received 28 September 2011
Accepted 4 November 2011
Available online 10 November 2011

Keywords:
Stainless steel
Ion implantation
Corrosion resistance

ABSTRACT

The effects of titanium ion implantation on the surface chemical composition, roughness, and microstructure, as well as corrosion mechanism of 316L stainless steel in acid solution are investigated. The bare SS316L has a polycrystalline structure containing second-phase inclusions. These defects are prone to pitting corrosion and intergranular corrosion as observed by SEM. After Ti ion implantation, the outer surface is completely amorphized and homogenized and the region underneath is partly disordered. Consequently, localized corrosion is avoided and the sample undergoes general corrosion. With increasing ion implantation voltages, the surface roughness increases and the corrosion resistance decreases due to more extensive radiation damage as result of energetic ion bombardment.

1. Introduction

Stainless steels are used in a myriad of applications due to their relatively low cost and reasonable corrosion resistance [1]. The good corrosion resistance results from the presence of a thin passive film on its surface typically about several nanometers thick [2]. Nevertheless, stainless steels are susceptible to local corrosion mainly due to the compositional difference and second-phase inclusions such as manganese sulfide [3]. In traditional metallurgical techniques, the composition range of the bulk materials is limited by precipitation of intermetallic phases and the inclusions cause defects in the passive film. The localized dissolution of stainless steels in an aggressive environment is one of the most common and catastrophic reasons for materials failure and hence, surface modification methods have been proposed to reduce or preclude localized corrosion and extend the service lifetime [4].

Ion implantation is widely used to introduce different elements into the surface of materials due to the high productivity, reproducibility, and low temperature [5–8]. The process can yield desirable surface properties such as wear resistance and corrosion resistance while the physical and mechanical stability of the bulk materials is not compromised [6]. Since ion implantation can in principle introduce any elements into the surface of the substrate to selected depths and concentrations forming alloys not restricted by the phase diagram [8], special alloys that retard corrosion can be formed on the surface. Titanium and its alloys have good corrosion resistance in acidic and humid conditions even at high positive overpotentials [9]. The present work aims at investigating the effects of Ti ion implantation at different voltages on the surface topography, composition, structure, and corrosion behavior of SS316L in an acidic medium.

2. Experimental details

Austenitic 316L stainless steel was used in our experiments. Ion implantation was carried out on the HEMII-80 High Energy Metal Ion Implanter. Titanium was implanted at accelerating voltages of 20, 40, 60, and 80 kV and the nominal ion implantation fluence was about 2×10^{17} ions cm^{-2}. The vacuum in the implantation chamber was below 5.0×10^{-5} Pa.

X-ray photoelectron spectroscopy (XPS) was conducted on a Kratos AXIS Ultra with a monochromated Al K_α radiation source. The surface topography was measured by atomic force microscopy (AFM) and transmission electron microscopy (TEM) was used to observe the microstructures in the bare and Ti implanted SS316L. The surface topography after the electrochemical tests was also examined by SEM. The electrochemical tests were carried out in 0.5 M H_2SO_4 + 2 ppm HF solution at 80 °C. The potential is referred to saturated calomel electrode (SCE).

3. Results and discussion

As shown in Fig. 1(a), the passive film on the control about 3 nm thick is composed of predominantly iron and chromium oxides, whereas the region closest to the metal/film interface (3–5 nm) is rich in nickel. After 20 kV Ti ion implantation, the titanium concentration is significantly increased. A titanium rich layer with a thickness of about 100 nm is formed in the near-surface region and the peak atomic fraction of Ti is about 55% at a depth of 12 nm. It is noted that the iron concentration diminishes greatly but that of chromium

* Corresponding authors. Tel.: +86 21 54748940; fax: +86 21 62182903.
E-mail addresses: xcai@sjtu.edu.cn (X. Cai), lizg@sjtu.edu.cn (Z. Li).

0167-577X/$ – see front matter.
doi:10.1016/j.matlet.2011.11.014

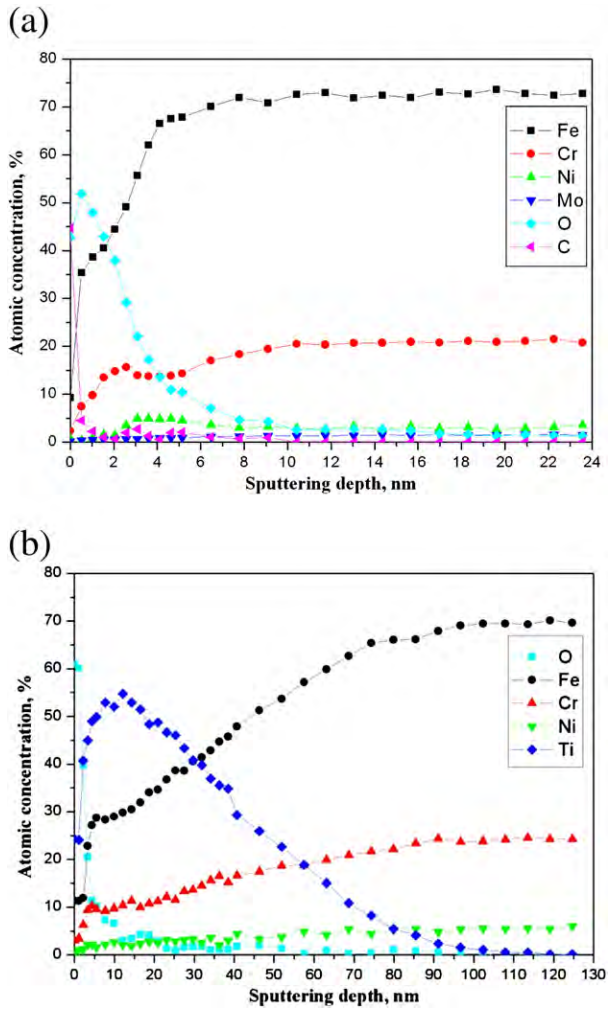

Fig. 1. XPS depth profiles acquired from (a) bare SS316L, and (b) Ti implanted sample with an accelerate voltage of 20 kV.

is almost the same, indicating that the concentration of iron in the implanted layer is replaced by titanium.

Fig. 2(a)–(d) depicts the surface topography of the SS316L samples implanted at 20, 40, 60, and 80 kV, respectively. The surface roughness increases with the ion implantation voltage. According to Fig. 2(a) and (b), the difference between 20 kV and 40 kV is not obvious, although there are some fringes on the surface due to mechanical polishing. However, at 60 kV and 80 kV, the surface becomes much rougher and the roughness overwhelms these fringes. 60 kV appears to be the threshold when significant surface roughening occurs.

The substrate is identified as austenite (γ-phase) and possesses a polycrystalline structure with a grain size of about 10 μm as indicated by Fig. 3(a) and (b). There are second-phase inclusions and dislocations inside the grain. These defects may become metastable pits for the initial point of local corrosion. Fig. 3(c) shows the cross-section of the 20 kV Ti implanted sample disclosing a 15 nm thick amorphous layer on the surface, indicating that at 20 kV, a fluence of 2×10^{17} ions cm^{-2} is sufficient to amorphize the surface. Between 20 nm and 100 nm, the dark areas show an orderly structure indicating crystallinity in spite of radiation damage. Therefore, the layer is only partially damaged in this region.

The polarization curves in Fig. 4(a) reveal a self-passivation behavior in all the samples. The corrosion potential of SS316L is about −0.28 V and the passivation region starts from −0.1 V to 0.85 V. When the potential is higher than 0.85 V, the corrosion current density of SS316L increases dramatically due to transpassivation of the passive film. Titanium does not exhibit a transpassive behavior in the higher potential region due to its good corrosion resistance at high positive overpotentials. The corrosion potential of the Ti implanted SS316L is higher than those of both the bare SS316L and pure titanium and it increases with implantation voltage. The passivation behavior is more similar to that of pure titanium showing no peak passivating current and slowly increasing passivation current density. It is reasonable on account of the high ion implantation fluence of 2×10^{17} ions cm^{-2} subsequently giving rise to a peak Ti concentration of almost 55% as revealed by XPS. However, the Ti implanted samples exhibit a transpassive behavior and the transpassivation potential of 0.95 V is more positive than that of the bare control. The passivation current density of Ti implanted SS316L

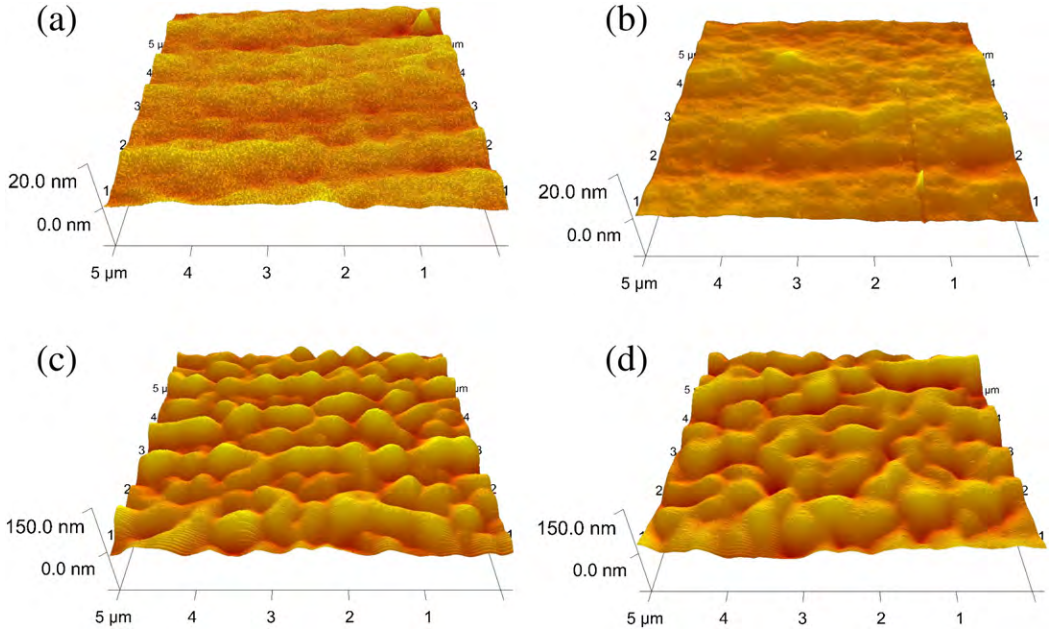

Fig. 2. AFM 3D image (tapping mode) of the SS316L implanted at different voltages: (a) 20 kV, (b) 40 kV, (c) 60 kV, and (d) 80 kV.

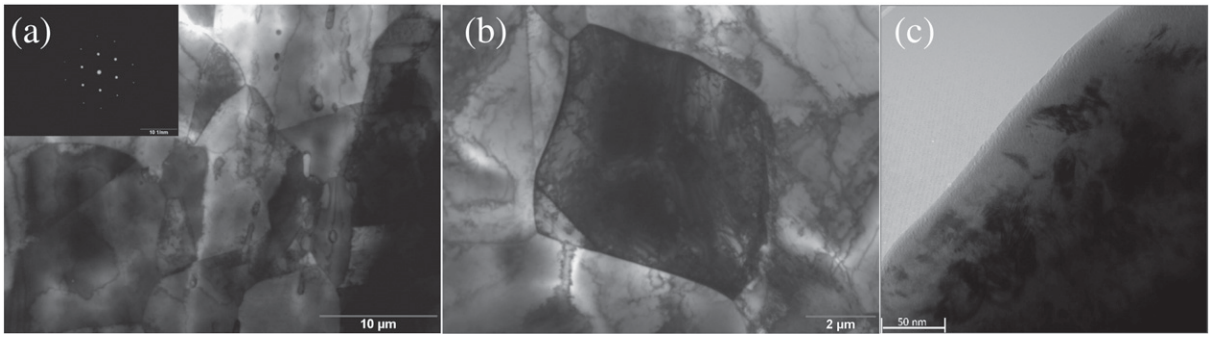

Fig. 3. TEM bright-field image and selected area diffraction (SAD) patterns of (a), (b) SS316L and (c) cross-section of the microstructure in the 20 kV Ti implanted SS316L.

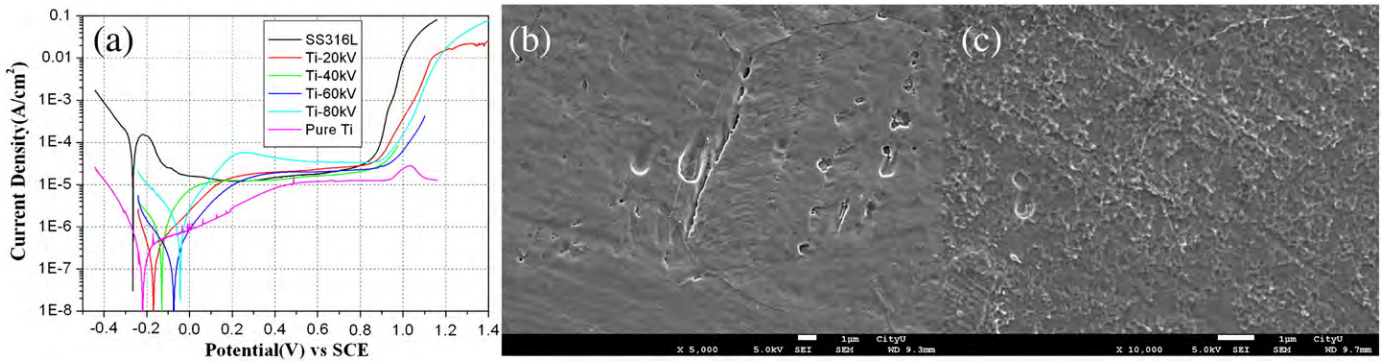

Fig. 4. (a) Potentiostatic curves of the bare and Ti implanted SS316L, (b) SEM images of the surface topography of the bare SS316L after polarization, and (c) surface topography of ion implanted SS316L after polarization.

increases with ion implantation voltage. As indicated by the AFM results, the higher the implantation voltage, the more severe is radiation damage which creates defects which are more susceptible to corrosion. It is also known that the roughness of the surface affects pitting corrosion especially in the early stage [10]. The bare SS316L undergoes serious pitting corrosion and intergranular corrosion as shown in Fig. 4(b). The local corrosion arises from the compositional difference and defects in the grain boundary as shown in Fig. 3(b) as well as second-phase inclusions shown in Fig. 3(a). The pitting corrosion is triggered by the unusually fast dissolution of inclusions which are less stable against dissolution because of the presence of Fe and Fe/Cr rich phases in the inclusions. The intergranular corrosion shown in Fig. 4(b) stems from the chromium-depleted zone around the grain boundary caused by precipitation of chromium carbides. However, the ion implanted SS316L exhibits general corrosion instead of local corrosion. There are many small corrosion cells which are shallow and stable as shown in Fig. 4(c). This is because the surface of the ion implanted SS316L is amorphous (Fig. 3 (c)) and it affects the surface corrosion mechanism.

4. Conclusion

After Ti ion implantation, a titanium rich layer about 100 nm thick is formed in the near-surface region with a peak atomic fraction of 55% at a depth of 12 nm. The surface roughness increases with implantation voltage due to more severe radiation damage at higher implantation voltages. The microstructure of SS316L is polycrystalline with a grain size of about 10 μm together with inherent second-phase inclusions and dislocations. These defects are prone to initial pitting corrosion and intergranular corrosion as confirmed by SEM after polarization. Potentiodynamic tests show that, as the implantation voltage increases, the passivation current density increases due to more radiation damage and rougher surface. Our results indicate that although Ti ion implantation improves the corrosion resistance of SS316L, an implantation voltage that is too high leads to worse results.

Acknowledgments

Financial support from the National Natural Science Foundation of China under contract number 50820125506 and No.50971091, National High Technology Research and Development Program 863 under contract number 2009AA05Z120, the Ministry of Science and Technology of the People's Republic of China (Grant No.2009DFB50350), Hong Kong Research Grants Council (RGC) General Research Funds (GRF) No. CityU 112608 is acknowledged.

References

[1] Chabica ME, Williamson DL, Wei R, Wilbur PJ. Surf Coat Technol 1992;51:24.
[2] Olsson COA, Landolt D. Electrochim Acta 2003;48:1093.
[3] Ryan MP, Williams DE, Chater RJ, Hutton BM, McPhall DS. Nature 2002;415:770.
[4] Abreu CM, Cristobal MJ, Fifueroa R, Merino P, Pena G, Perez MC. Surf Interface Anal 2010;42:621.
[5] Wu G, Gong L, Feng K, Wu S, Zhao Y, Chu PK. Mater Lett 2011;65:661.
[6] Sugizaki Y, Yasunaga T, Tomari H. Surf CoatTechnol 1996;83:167.
[7] Chu PK. Surf CoatTechnol 2010;204:2853.
[8] Sharkeen YP, Gritsenko BP, Fortuna SV, Perry AJ. Vacuum 1999;52:247.
[9] Jung HY, Huang SY, Ganesan P, Popov BN. J Power Sources 2009;194:972.
[10] Stimming U. Electrochim Acta 1986;31:415.